

Theory of carrier concentration-dependent electronic behavior in layered cobaltates

H. Li,¹ R. T. Clay,² and S. Mazumdar¹

¹*Department of Physics, University of Arizona, Tucson, AZ 85721*

²*Department of Physics and Astronomy and HPC Center for Computational Sciences,
Mississippi State University, Mississippi State, MS 39762*

(Dated: March 29, 2011)

A natural explanation for the carrier concentration-dependent electronic behavior in the layered cobaltates emerges within correlated-electron Hamiltonians with finite on-site and significant nearest neighbor hole-hole Coulomb repulsions. The nearest neighbor repulsion decreases hole double-occupancy below hole density $\frac{1}{3}$, but increases the same at higher hole densities. Our conclusion is valid for both single-band and three-band extended Hubbard Hamiltonians, and sheds light on concentration-dependent e'_g hole occupancy within the latter.

PACS numbers: 71.10.Fd, 71.10.Hf, 74.20.Mn, 74.70.Kn

Layered cobaltates – anhydrous Na_xCoO_2 , Li_xCoO_2 and the misfit cobaltates $[\text{Bi}_2\text{A}_2\text{O}_4][\text{CoO}_2]_m$, where A = Ba, Sr or Ca and m is incommensurate – have attracted wide attention for their unconventional metallicity and tunability of the carrier concentration. Na_xCoO_2 consists of edge-sharing CoO_6 octahedra, with CoO_2 layers separated by Na layers. The Co ions with average charge $(4-x)+$ form a triangular lattice. Both experiments [1] and theory [2] indicate large crystal-field splitting and therefore low-spin states for the Co-ions. Trigonal distortion splits the t_{2g} d -orbitals into two low-lying e'_g orbitals and a higher a_{1g} orbital. Charge carriers are $S = \frac{1}{2}$ holes on the Co^{4+} ion sites [3]. The hole density $\rho = 1 - x$ in anhydrous Na_xCoO_2 and Li_xCoO_2 . Angle-resolved photoemission from Na_xCoO_2 indicate that carriers occupy the a_{1g} orbitals only [3–5], although Compton scattering finds small x -dependent e'_g contribution [6].

The electronic and magnetic behavior of these materials exhibit a peculiar carrier concentration-dependence. The temperature-dependent magnetic susceptibility $\chi(T)$ in Na_xCoO_2 was early on characterized as “Pauli paramagnetic” for $x < 0.5$ and “Curie-Weiss” for $x > 0.5$ [7]. The Curie-Weiss behavior reflects strong Coulomb repulsion between the holes [1, 3, 4, 7, 8]. Strong correlation at large x is supported by observations of charge-ordering (CO) [9, 10], Na-ion ordering [11], spin-density wave and intralayer ferromagnetic correlations [12]. Qualitatively different behavior for the small x region is also agreed upon. Recent experimental work suggest that (a) $\chi(T)$ here is weakly antiferromagnetic rather than Pauli paramagnetic, and (b) the cross-over between strong and weak correlations occurs at $x \sim 0.63 - 0.65$ rather than $x = 0.5$ [10]. CO and Na-ion ordering are both absent for small x [10].

Understanding the x -dependence of the electronic and magnetic behavior of Na_xCoO_2 continues to be a theoretical challenge. It has been suggested that while the a_{1g} -only description is valid for large x , holes occupy both a_{1g} and e'_g orbitals at small x [13], and the on-site Hubbard correlation U is x -dependent. Quantum

chemical configuration interaction calculations [14] find larger $a_{1g} - e'_g$ separation than LDA calculations [2], and (ii) many-body approaches that take Coulomb hole-hole repulsion into account [15–17] do not find the e'_g pockets on the Fermi surface predicted within LDA calculations. x -dependence has also been ascribed to differences in the potential due to Na layers [11, 18]. Experimentally, Li_xCoO_2 [19] and Bi “misfit” cobaltates [20] do not exhibit ion ordering but nevertheless exhibit very similar carrier concentration-dependence [19, 20], suggesting that this dependence is *intrinsic to the CoO₂ layers*, with the interlayer potential playing a secondary role.

In the present Letter we show that a simple and natural explanation of the carrier concentration-dependence emerges within a_{1g} -only as well as multiband extended Hubbard models. As we will be interested in all three families of layered cobaltates including the misfits, henceforth our discussions involve ρ which is well-defined for all systems, instead of x . Following [16] we write the three-band Hamiltonian as

$$H = - \sum_{\langle ij \rangle \alpha \beta \sigma} t_{\alpha \beta} c_{i \alpha \sigma}^\dagger c_{j \beta \sigma} + \sum_i \Delta (n_{i e'_g} - n_{i a_{1g}}) + \frac{1}{2} \sum_{i \alpha \beta \sigma \sigma'} U_{\alpha \beta}^{\sigma \sigma'} n_{i \alpha \sigma} n_{i \beta \sigma'} + V \sum_{\langle ij \rangle \alpha \beta} n_{i \alpha} n_{j \beta}. \quad (1)$$

Here α and β refer to the a_{1g} and e'_g orbitals, $c_{i \alpha \sigma}^\dagger$ creates a hole of spin σ on orbital α on site i , $n_{i \alpha \sigma} = c_{i \alpha \sigma}^\dagger c_{i \alpha \sigma}$ and $n_{i \alpha} = \sum_\sigma n_{i \alpha \sigma}$. $t_{\alpha \beta}$ is the nearest neighbor (n.n.) hopping, Δ the trigonal splitting, $U \equiv U_{\alpha \alpha}^{\sigma \sigma}$ and $U' \equiv U_{\alpha \beta}^{\sigma \sigma'}$ are the onsite intra- and inter-orbital Coulomb interactions, and V is the n.n. Coulomb interaction. As in [16], we have ignored the Hund’s rule coupling based on the very small hole occupation of e'_g orbitals (see below). As both photoemission experiments [3–5] and many-body theories [14, 15, 17] find negligible role of e'_g orbitals, we discuss the one-band limit of Eq. 1 first. We show that the V term is essential within the one-band model for understanding the ρ dependence of the susceptibility. We then show that the same effect not only persists in the

full three-band model, but influences the ρ -dependence of the e'_g orbital occupation as well.

Single-band limit. Terms containing U' and Δ are irrelevant and U , V , and $t_{\alpha\alpha}$ refer to a_{1g} orbitals only. We write $t_{\alpha\alpha} = t$ and express U and V in units of t . For hole carriers $t > 0$ [3]. Existing a_{1g} -only theories largely assume $U \gg t$ [21] or $V = 0$ [15, 17, 18, 21, 22]. The few studies that have investigated the effects of finite V on triangular lattices are either for particular $\rho = 0.5$ [23] or $\frac{2}{3}$ [24], or use approximate approaches [25] that do not capture the complex ρ -dependence that is seen experimentally and that we find in our exact solutions. We consider here realistic finite U and V and investigate all ρ . We do not assume that U and V are ρ -dependent. Rather, we show that ρ -dependent correlations emerge as solutions to Eq. 1.

Two different observations give the appropriate parameter range. (i) At $\rho = 1$ Eq. 1 can be replaced by a $V = 0$ Hubbard Hamiltonian with an *effective* on-site repulsion $U_{\text{eff}} = U - V$. Within the $V = 0$ Hubbard model for the triangular lattice, transition to the Mott-Hubbard insulator occurs for $U_{\text{eff}} > U_c$, where $U_c \simeq 5 - 10$. [26]. Experimentally, $\rho = 1$ CoO₂ is a poor metal close to the Mott-Hubbard transition [8], indicating that $U - V \leq 5 - 10$ for cobaltates. (ii) For $V > \frac{1}{3}U$, $\rho = \frac{2}{3}$ would be charge-ordered with all sites doubly occupied (Co⁵⁺) and vacant (Co³⁺), as shown in Fig. 1(d). The absence of such CO indicates $V < \frac{1}{3}U$. Taking (i) and (ii) together, we conclude that the likely parameter regime is $6 < U < 14$, $1 < V < 4$. Our estimate of V/U is close to that of Choy *et al.* [23]. Our estimate of U/t is slightly smaller [13, 17].

We now argue that for realistic U and V there occur three distinct hole density regions. (i) $\rho \leq \frac{1}{3}$, where correlation effects are strongest; (ii) intermediate $\frac{1}{3} < \rho \leq \frac{2}{3}$, where correlation effects become weaker with increasing density, and can be quite weak at the highest ρ ; and (iii) $\rho > \frac{2}{3}$, where correlation effects increase again slowly. We classify configurations by the number of double occupancies N_d . Fig. 1 (a) shows the $\sqrt{3} \times \sqrt{3}$ $N_d = 0$ charge-ordered configuration that should dominate the ground state of $\rho = \frac{1}{3}$. For fixed U , nonzero V creates an energy barrier to holes approaching each other. The effective energy cost of creating a double occupancy is thus *greater than* U for $\rho \leq \frac{1}{3}$, which should exhibit strongly correlated behavior. This situation changes as ρ increases, as seen in Fig. 1 (b), where we have added a single hole to the charge-ordered configuration of $\rho = \frac{1}{3}$. The particular hop indicated in the figure that creates a double occupancy costs only $U - 3V$. There are only three of these, and they increase $\langle N_d \rangle$ very slightly. With further increase in ρ , the number of these low energy hops increases rapidly, increasing $\langle N_d \rangle$. In Fig. 1(c) we show the two extreme charge-ordered configurations for $\rho = \frac{2}{3}$, one with $N_d = 0$ (Fig. 1(c)), the other with $N_d = N_{\text{max}} = \frac{1}{3}N$. The configurations are degenerate at $U = 3V$. *There is*

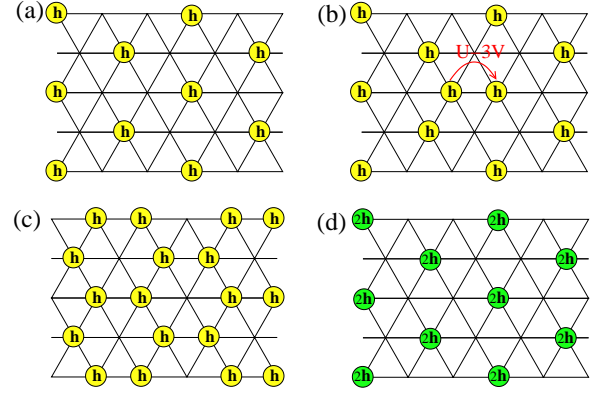


FIG. 1: (Color online) Dominant ground state configurations for (a) $\rho = \frac{1}{3}$ and (b) one hole added to $\rho = \frac{1}{3}$. Circles labeled 'h' ('2h') are singly (doubly) occupied sites, with vacancies occupying the vertices of the triangular lattice. The n.n. hop indicated by the arrow in (b) costs $U - 3V$. Dominant configurations for $\rho = \frac{2}{3}$, with (c) $N_d = 0$, and (d) $N_d = \frac{1}{3}N$.

thus strong mixing of $N_d = 0$ and $N_d > 0$ configurations for ρ close to $\frac{2}{3}$, even for $V < \frac{1}{3}U$. Adding double occupancies to the configuration in Fig. 1(d) is prohibitively expensive in energy, which implies that for $\rho > \frac{2}{3}$ the competition of $N_d = 0$ is no longer with $N_d = N_{\text{max}}$ but still with $N_d = \frac{1}{3}N$. We expect correlations to slowly increase again in this region.

We have performed exact numerical calculations to confirm the above conjectures. As a measure of correlations we have chosen the normalized probability of double occupancy $g(\rho)$ in the ground state,

$$g(\rho) = \frac{\langle n_{i,\uparrow} n_{i,\downarrow} \rangle}{\langle n_{i,\uparrow} \rangle \langle n_{i,\downarrow} \rangle} \quad (2)$$

$g(\rho) = 1$ and 0 for $U = 0$ and $U \rightarrow \infty$, respectively, for all ρ , and has intermediate values in between. $g(\rho)$ is thus a measure of $U_{\text{eff}}(\rho)$: small $g(\rho)$ implies enhanced Curie-Weiss type $\chi(T)$ while moderate to large $g(\rho)$ implies weak antiferromagnetic spin-spin correlations [27]. Our proposed mechanism suggests that $g(\rho)$ is small (large) for small (large) hole density, provided V is significant.

We have calculated g for the six triangular lattice clusters in Fig. 2, using periodic boundary condition. For clusters (a)-(c) the number of holes N_h covers the complete range $\rho \leq 1$. Computer memory constraints restrict us to $\rho \leq 0.88$ for cluster (d) and $\rho \leq 0.6$ for clusters (e) and (f), respectively. Our calculations are for all realistic U and $V \leq \frac{1}{3}U$. As the results are qualitatively the same in all cases, we report our results for $U = 10$ only.

In Fig. 3 we show our results for clusters (a)-(d) for $U = 10$ and $V = 0, 2$ and 3. Our data points include both even and odd N_h , and except for $N_h \geq 14$ in Fig. 3(d) we have determined the total spin S in the ground state in each case. With few exceptions, $S = S_{\text{min}}$, with $S_{\text{min}} = 0$ ($\frac{1}{2}$) for even (odd) N_h . $S > S_{\text{min}}$ is a finite-size effect,

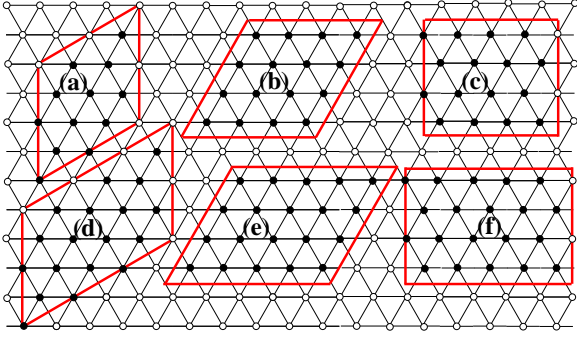


FIG. 2: (Color online) Clusters investigated numerically: (a) $N = 12$; (b) and (c) $N = 16$; (d) $N = 18$; (e) and (f) $N = 20$

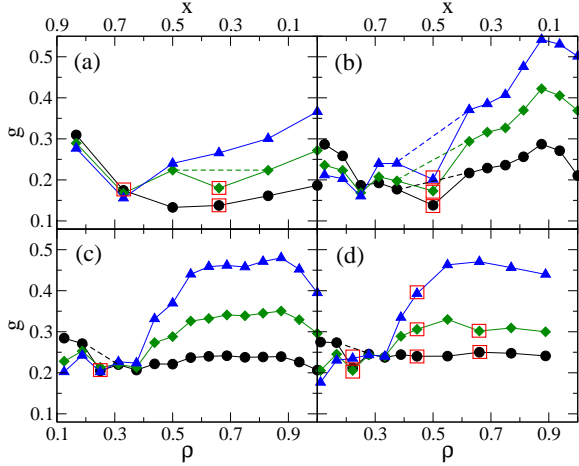


FIG. 3: (Color online) Normalized probability of double occupancy of sites by holes versus hole density for $U=10$, $V=0$ (circles), 2 (diamonds) and 3 (triangles) on clusters with (a) $N = 12$, (b) and (c) $N = 16$, corresponding to Fig. 2(b) and (c), respectively, and (d) $N = 18$. Points within squares indicate $S > S_{\min}$ (see text).

as for different clusters this occurs at different densities. The g -values for the $S > S_{\min}$ points were calculated correctly in accordance with Eq. 2. The dips in g for higher S are expected. In every case we have included dashed straight lines connecting the neighboring points on both sides. The g for $S = S_{\min}$ at these points is likely bounded by the computed points and the dashed lines.

In all four cases in Fig. 3, $g(\rho)$ is nearly independent of ρ for $V = 0$, but exhibits the ρ -dependence predicted for $V \neq 0$. The ρ -dependence is weakest for $N = 12$. In all other cases there occur distinct strongly correlated low density region ($\rho \leq 0.4$), where V suppresses g and relatively weakly correlated intermediate density region ($0.4 \leq \rho \leq 0.8$), where V enhances g . The predicted decrease in $g(\rho)$ for larger ρ is also visible in Fig. 3(b) and (c).

Fig. 4 shows plots of $g(\rho)$ for the 20-site clusters of Fig. 2(e) and (f). As in Fig. 3 we have retained the points with $S > S_{\min}$. *Distinct density regions (i) and*

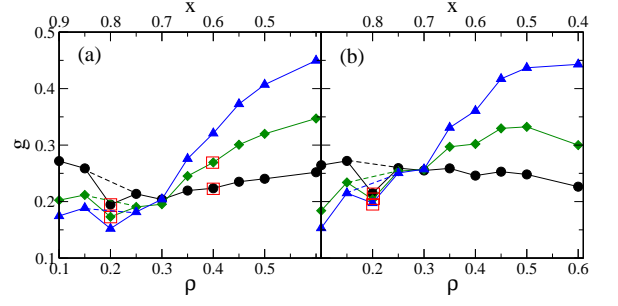


FIG. 4: (Color online) Same as Fig. 3 for $N = 20$, for $U = 10$ and $V = 0$ (circles), 2 (diamonds) and 3 (triangles); (a) and (b) correspond to lattices Fig. 2(e) and 2(f), respectively.

(ii), with opposite effects of V are again clearly visible. The boundary between strongly and weakly correlated regions is $\rho \approx 0.30$, in agreement with recent experiments [10]. Calculated charge-charge correlations $\langle n_i n_j \rangle$ (not shown) indicate that while near $\rho = \frac{1}{3}$ ($N_h = 6$ and 7) there is tendency to CO there is no such tendency at $\rho = 0.5$ ($N_h = 10$). The qualitative agreement between our results for six different clusters, *along with steeper ρ -dependence with increasing N* , strongly suggest that our results will persist in the thermodynamic limit.

Three-band model. ρ -dependent g is a consequence of the competition between U and V at large ρ [27] and is unrelated to dimensionality or frustration. Since exact calculations are not possible for the clusters of Fig. 2 within the three-band model, we have performed three-band calculations for a one-dimensional (1D) periodic cluster with eight sites, each with one “ a_{1g} ” and two “ e'_g ” (hereafter a , e_1 and e_2 , respectively) orbitals. The only differences between 1D and the triangular lattice are, (i) the Wigner crystal occurs at $\rho = \frac{1}{2}$ in 1D instead of $\rho = \frac{1}{3}$, and (ii) the maximum in $g(\rho)$ is expected near $\rho = \frac{3}{4}$ [27] rather than $\frac{2}{3}$. We retain the same U and V as for the single-band model. We have taken $t_{\alpha\alpha} = t$, and inter-orbital hopping $t_{\alpha\beta} = 0.1 - 0.3t$ ($\alpha \neq \beta$), $\Delta = 3|t|$ [14], and $U' = 0.6U$ [17]. As is common for 1D rings, we use periodic (anti-periodic) boundary conditions for $N_h = 4n + 2$ ($4n$) [28].

In Fig. 5(a), we have plotted $g_a(\rho)$, the normalized probability of double occupancy of the a -orbitals by holes, within the three-band model ($g_e(\rho)$ varies by less than 15% over the entire range of ρ). The carrier density ρ here is the ratio of the total number of holes and the number of a -orbitals, in agreement with the definition of ρ in Na_xCoO_2 . The $g_a(\rho)$ -behavior is nearly identical to that of $g(\rho)$ in Figs. 3 and 4. Interestingly, $g_a(\rho)$ behavior is the same for small and large $t_{e,a}$, *in spite of moderate hole population $n(e)$ in the e orbitals in the latter case*. Calculations for smaller Δ (not shown) indicate similar weak dependence of $g_a(\rho)$ on Δ .

In Fig. 5(b) we plot $r(e)$, the fraction of holes that occupy the e orbitals, assuming $t_{\alpha\beta} = 0.3t$, for (a) non-

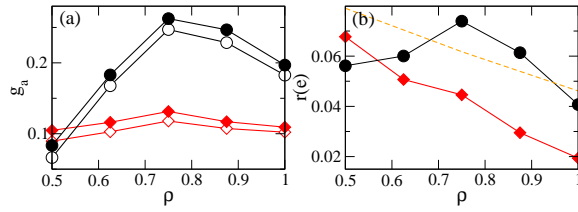


FIG. 5: (Color online) (a) Normalized probability of double occupancy of the a -orbitals by holes in the 1D 3-band model for $N = 8$, $\Delta = 3$ (b) The fraction of holes occupying e -orbitals. In both, unfilled (filled) symbols are for inter-orbital hopping $0.1t$ ($0.3t$). Diamonds (circles) are for $V = 0$ ($V = 3$). In (b), the dashed line shows the noninteracting ($U = U' = V = 0$) result. For all other points $U = 10$ and $U' = 6$.

interacting, (b) $U, U' \neq 0$ but $V = 0$, and (c) $V > 0$ cases. For $t_{\alpha\beta} = 0.1t$, $r(e) \lesssim 0.01$ and is negligible. Comparing the noninteracting and the $V = 0$ plots, it is clear that nonzero U and U' decrease the e'_g occupation, the reason for which can only be correlation-induced band narrowing [15, 17]. It is, however, the $V > 0$ plot that is far more interesting: $r(e)$ now shows a peak *at the same* ρ where $g_a(\rho)$ has a maximum. This shows that correlation effects due to V play a much more complex role in the multiband picture: in the large- ρ region V reduces U_{eff} (Fig. 5(a)) for the same reason as in the single-band picture. This reduces the extent of band-narrowing at precisely these ρ , and leads to an *increase* in $r(e)$ *even for ρ -independent* Δ . Existing discussions of e'_g hole occupancy have largely focused on the Fermi surface [3–6]. Our work shows that there can occur weak e'_g hole occupation even if only the a_{1g} -orbitals form the Fermi surface. Most interestingly, the e'_g occupation estimated by Compton scattering experiments shows a ρ -dependence (see Table I in [6]) that is very similar to our results for $V > 0$ in Fig. 5(b), viz., *increasing* e'_g -occupancy with increasing ρ . This result simply cannot be explained with $V = 0$, as seen in Fig. 5(b). Our calculations show that ρ -dependent $\chi(T)$ and e'_g occupation are manifestations of the same many-body effect.

Summary. Strongly correlated behavior for small hole densities and relatively weakly correlated behavior for larger hole densities are both expected for nonzero n.n. Coulomb interaction. To the best of our knowledge there exists no other satisfactory theoretical explanation for the observed weakly correlated behavior nearer to the Mott-Hubbard semiconducting hole density and strongly correlated behavior farther away from this limit. The strong tendency to CO at ρ exactly $\frac{1}{3}$ and the absence of this tendency at $\rho = \frac{2}{3}$ are both understood. The potential due to Na-ions, ignored in our work, will strengthen the CO even for incommensurate fillings with $\rho \leq \frac{1}{3}$ [11]. We do not find CO at $\rho = 0.5$, although it is moderately correlated. Observed CO here [7] is likely driven by the cooperative effects of V and the Na-ion potential.

Conversely, the absence of Na-ion ordering for weakly correlated $x < 0.5$ in Na_xCoO_2 further suggests that the CO and Na-ion ordering are synergistic effects.

This work was supported by the Department of Energy grant DE-FG02-06ER46315.

-
- [1] Y. Wang et al., Nature **423**, 425 (2003); T. Mizokawa, New J. Phys. **6**, 169 (2004).
 - [2] D. J. Singh, Phys. Rev. B **61**, 13397 (2000).
 - [3] M. Z. Hasan et al., Phys. Rev. Lett. **92**, 246402 (2004).
 - [4] H.-B. Yang et al., Phys. Rev. Lett. **95**, 146401 (2005).
 - [5] D. Qian et al., Phys. Rev. Lett. **96**, 216405 (2006).
 - [6] J. Laverock et al., Phys. Rev. B **76**, 052509 (2007).
 - [7] M. L. Foo et al., Phys. Rev. Lett. **92**, 247001 (2004).
 - [8] C. de Vaulx et al., Phys. Rev. Lett. **98**, 246402 (2007).
 - [9] I. R. Mukhamedshin et al., Phys. Rev. Lett. **94**, 247602 (2005).
 - [10] G. Lang et al., Phys. Rev. B **78**, 155116 (2008).
 - [11] M. Roger et al., Nature **445**, 631 (2007); G. J. Shu et al., Phys. Rev. B **82**, 054106 (2010).
 - [12] S. P. Bayrakci et al., Phys. Rev. Lett. **94**, 157205 (2005). L. M. Helme et al., *ibid* **94**, 157206 (2005).
 - [13] K.-W. Lee and W. E. Pickett, Phys. Rev. B **72**, 115110 (2005).
 - [14] S. Landron, J. Soret, and M.-B. Lepetit, J. Phys. Condens. Matter **22**, 345603 (2010).
 - [15] S. Zhou et al., Phys. Rev. Lett. **94**, 206401 (2005).
 - [16] C. A. Marianetti, K. Haule, and O. Parcollet, Phys. Rev. Lett. **99**, 246404 (2007).
 - [17] A. Bourgeois, A. A. Aligia, and M. J. Rozenberg, Phys. Rev. Lett. **102**, 066402 (2009).
 - [18] C. A. Marianetti and G. Kotliar, Phys. Rev. Lett. **98**, 176405 (2007).
 - [19] T. Motohashi et al., Phys. Rev. B **80**, 165114 (2009).
 - [20] J. Bobroff et al., Phys. Rev. Lett. **96**, 107201 (2006); V. Brouet et al., Phys. Rev. B **76**, 100403(R) (2007).
 - [21] G. Baskaran, Phys. Rev. Lett. **91**, 097003 (2003); B. Kumar and B. S. Shastry, Phys. Rev. B **68**, 104508 (2003); O. I. Motrunich and P. A. Lee, Phys. Rev. B **69**, 214516 (2004); J. O. Haerter, M. R. Peterson, and B. S. Shastry, *ibid* **97**, 226402 (2006); W.-H. Wang et al., J. Phys.: Condens. Matter **21**, 205602 (2009).
 - [22] J. Merino, B. J. Powell, and R. H. McKenzie, Phys. Rev. B **79**, 161103 (2009); B. J. Powell, J. Merino, and R. H. McKenzie, *ibid* **80**, 085113 (2009); F. Lechermann et al., Phys. Rev. Lett. **102**, 046403 (2009).
 - [23] T. P. Choy, D. Galanakis, and P. Phillips, Phys. Rev. B **75**, 073103 (2007).
 - [24] H. Watanabe and M. Ogata, J. Phys. Soc. Jpn. **74**, 2901 (2005).
 - [25] B. Davoudi, S. R. Hassan, and A.-M.S. Tremblay, Phys. Rev. B **77**, 214408 (2008); S. R. Hassan and L. de' Medici, Phys. Rev. B **81**, 035106 (2010); C. Piefke, L. Beohnke, A. Georges, and F. Lechermann, Phys. Rev. B **82**, 165118 (2010).
 - [26] T. Mizusaki and M. Imada, Phys. Rev. B **74**, 014421 (2006); D. Galanakis, T. D. Stanescu, and P. Phillips, *ibid* **79**, 115116 (2009); B. Kyung and A. -M. S. Tremblay, Phys. Rev. Lett. **97**, 046402 (2006).
 - [27] S. Mazumdar and S. N. Dixit, Phys. Rev. B **34**, 3683

(1986).

[28] See supplementary information EPAPS-xxxx.